JOURNAL OF AIRCRAFT
Vol. 30, No. 2, March–April 1993

Measurements of Aerodynamic Rotary Stability Derivatives Using a Whirling Arm Facility

Marc J. M. Mulkens* and Albert O. Ormerod*
Cranfield Institute of Technology, Cranfield, Bedfordshire MK 43 OAL, England, United Kingdom

This work is part of a program of research in which the high angle-of-attack region is of particular interest. Equipment and methods have been developed to adapt a whirling arm facility for the measurement of the effects of path curvature on two generic combat aircraft configurations. An explanation is given of the merits of using a whirling arm and some of the difficulties are mentioned. The derivatives associated with steady rotation have been assessed at angles of attack up to 30 deg. Both longitudinal and directional tests have been made and comparisons with the results of oscillatory tests are presented. For the directional results, little difference was found. The longitudinal results, however, showed a significant difference at certain high angles of attack. These differences, which were of different signs for the two models tested, have to be attributed to effects associated with the rate of change-of-incidence.

Nomenclature

b = wing span
C_l = $L/(\frac{1}{2}\rho V^2 Sb)$
C_m = $M/(\frac{1}{2}\rho V^2 S\bar{c})$
C_n = $N/(\frac{1}{2}\rho V^2 Sb)$
C_{l_r} = $\partial C_l/\partial(rb/2V)$
$C_{l_{\dot\beta}}$ = $\partial C_l/\partial(\dot\beta b/2V)$
C_{m_q} = $\partial C_m/\partial(q\bar{c}/V)$
$C_{m_{\dot\alpha}}$ = $\partial C_m/\partial(\dot\alpha\bar{c}/V)$
C_{n_r} = $\partial C_n/\partial(rb/2V)$
$C_{n_{\dot\beta}}$ = $\partial C_n/\partial(\dot\beta b/2V)$
$\bar{c}$ = mean aerodynamic chord of the main wing
L = rolling moment
M = pitching moment
N = yawing moment
q = pitching angular velocity
R = whirling arm radius
$Re_{\bar{c}}$ = Reynolds' number based on $\bar{c}$
r = yawing angular velocity
S = wing area
t = time
V = airspeed
α = angle of attack
$\dot\alpha$ = $\partial\alpha/\partial t$
β = sideslip angle
$\dot\beta$ = $\partial\beta/\partial t$
ρ = air density
ω = angular velocity of the whirling arm

Subscripts
A = aerodynamic body axes
G = geometric body axes

Introduction

AN important aspect in the design of combat aircraft is the achievement of a high standard of maneuverability. This is required not only to avoid attacks from enemy aircraft or weapons, but also to get into a proper position for aiming weapons to be locked-on and released towards enemy targets. Thus, it is highly desirable for the aircraft to be able to fly tight turns in combat situations. The high-lift in maneuvers at low speeds necessitates flight at high angle of attack, often beyond the onset of flow separation over the upper wing surface. The aerodynamic phenomena in the range of angle of attack between flow separation and maximum lift needs to be well understood.

About 1980, the Royal Aircraft Establishment (RAE) started a program of research[1] on characteristics desirable for a modern combat aircraft and the production of representative mathematical models for suitable configurations. The program now involves free-flying models of two different configurations, designated HIRM I and HIRM II. (HIRM—high incidence research model) (see Fig. 1). HIRM I is a "three surface" configuration and HIRM II is a canard configuration without tailplanes and a higher swept main wing than HIRM I. To establish or justify data used in flight control systems for these models,[7] it is necessary to perform both static and dynamic wind-tunnel tests. For this purpose, a series of $\frac{4}{9}$ and $\frac{2}{9}$ scale models have been manufactured (full scale being defined as the free-flight model size), each being specifically built for dynamic or static testing.

A much-used method for dynamic wind-tunnel tests involves imposing an oscillatory motion on the model. Stability derivatives can be assessed from measurements of aerodynamic forces and moments using certain mathematical techniques. Usually, only composite derivatives can be derived in this way, e.g., $C_{m_q} + C_{m_{\dot\alpha}}$ for the longitudinal mode and $C_{n_r} - C_{n_{\dot\beta}} \times \cos(\alpha)$ and $C_{l_r} - C_{l_{\dot\beta}} \times \cos(\alpha)$ for the directional mode.

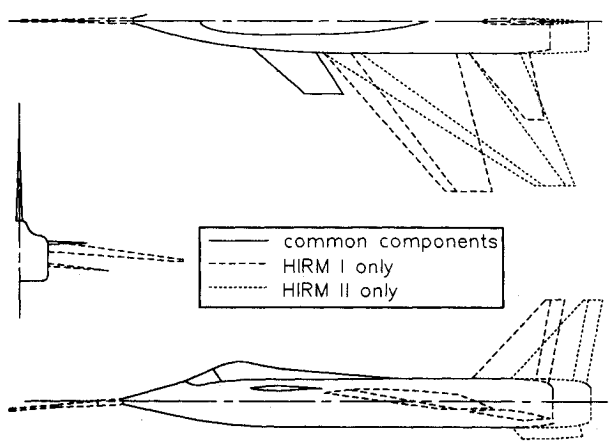

Fig. 1 HIRM I and HIRM II configurations.

Received July 30, 1991; revision received Jan. 13, 1992; accepted for publication Jan. 23, 1992.

*Research Assistant, Aerodynamics Department, College of Aeronautics.

Another way of investigating the aerodynamic effects of deviations from constant-speed rectilinear flight can be provided by a whirling arm on which a model is moved through the air at a constant incidence along a circular path. Trials have been made using the whirling arm facility of the Cranfield Institute of Technology to develop techniques for measuring the aerodynamic effects of steady rotation, covering the high-incidence regime, initially on HIRM I and then on HIRM II. It was considered possible to make measurements from which aerodynamic derivatives associated with a curved path could be obtained directly. This would include derivatives with respect to q in the longitudinal mode (such as C_{m_q}) and derivatives with respect to r in the directional mode (such as C_{l_r}). In principle, the associated cross-coupling derivatives could also be obtained. In spite of difficulties, worthwhile results were obtained from the whirling arm, complementing derivative measurements by other techniques and providing data which will eventually lead to a better understanding of the dynamics of maneuvers at high incidence.

Whirling Arm

Although several whirling arm facilities for aerodynamic experiments have been available in the past (e.g., Refs. 2 and 3), compared to wind tunnels their use has been limited. There were difficulties associated with their use which influenced the design of equipment and test procedures in the present work.

1) Swirl: This is the movement of air around the annular-shaped test passage as a result of drag of the model, the model-support and other moving parts of the whirling arm. This swirl is not a completely uniform flow around the test passage. Reference 5 gives results of an extensive investigation into swirl associated with the Cranfield whirling arm and describes modifications carried out to reduce swirl speed to about 5% of the model speed. Further effects of swirl during tests on the aircraft model, including the possible occurrence of flow into and out of the test passage through the inner-wall slot, are described in Ref. 6.

2) Centrifugal effects: High centrifugal forces influence the way models, strain gauge balances, and pressure measuring devices are designed and used. In the present tests these forces were about six times the gravitational force.

3) Low Reynolds' number: The maximum speed of the Cranfield whirling arm, with a size of model suitable for the derivative tests, gives a Reynolds' number ($Re_c = 5.8 \times 10^5$ for HIRM I) well below the values generally considered desirable for wind-tunnel tests. Thus, the whirling arm may not be suitable for tests where the flow over an aircraft model is critically sensitive to the test Reynolds' number.

The general layout of the whirling arm in use at the Cranfield Institute of Technology is given in Fig. 2. Originally installed at the National Physical Laboratory in 1942, it was re-erected at Cranfield in the early 1960s. Some general characteristics of the whirling arm are as follows:

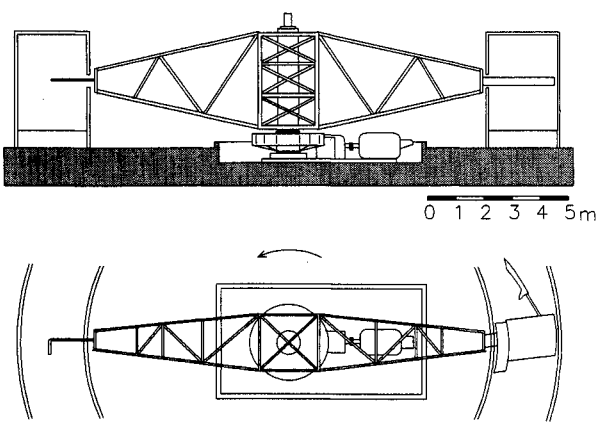

Fig. 2 General layout of the whirling arm.

1) The drive motor power is 53 kW. The motor is fed by up to 600 V dc supplied by a dedicated motor-generator set.

2) Maximum obtainable rotational speed is about 26.5 rpm, depending on the type of test-rig and model installed.

3) Test measurements are made with the arm rotating at a steady speed after a gradual acceleration from rest.

4) Rotation in an anticlockwise direction when viewed from above.

5) Test passage is a constant rectangular cross section whose width is 2.59 m and whose height is 3.40 m.

6) The radius (from arm center to center of the test passage) is 8.306 m.

7) The slot width is 0.75 m. (This is the gap in the inner wall of the test passage through which the model-support is connected to the arm.)

8) A timing device fed from an inductive sensor is used to measure the rate of rotation. A pitot-static tube mounted on the side of the arm opposite the model gives the relative airspeed. Combining the pitot-static information with the rate of rotation gives an indication of the speed of the air swirl in the test passage.

9) A hydraulically operated mechanism giving a rotation about a virtual axis through the model is used to move it between the attitudes at which steady-state data are acquired.

Models and Balance

The special models used in the whirling arm experiments are $\frac{4}{9}$ the scale of the free-flight models. One of the reasons for choosing this scale was that $\frac{4}{9}$ scale wind-tunnel models already existed and could be copied. The models have to be as light as possible to minimize the centrifugal loads acting on the internal strain gauge balance in combination with the aerodynamic loads. The weight of the models is only about 6 kg; the centrifugal force at 25 rpm of about 36 kg compares with an aerodynamic lift at $C_L = 1$ of the order 12 kg.

The models were built mainly from CRP (carbonfiber reinforced plastic), polyurethane foam, and glassfiber. A more detailed description can be found in Ref. 6.

For "wind-off" tests, to measure the centrifugal forces and moments without the aerodynamic forces and moments, a box-like cover, completely enclosing the model without touching it anywhere, was mounted on the sting behind the model.

The model-balance assembly is shown in Fig. 3. The special balance, designed to obtain the five components without axial force, does not conform to the usual wind-tunnel practice. The balance contains front and rear strain-gauge stations and, since the inertial loading systems acting on those stations are different, signals containing inertial effects cannot be combined electrically to represent the overall forces and moments. The adopted procedure was first to make wind-on and wind-off tests, determine the aerodynamic moments at each station by subtraction of wind-off from wind-on measurements, and then combine these to obtain the overall aerodynamic forces and moments.

As mentioned earlier, in order to increase the overall accuracy of the aerodynamic measurements, it is desirable to reduce, as far as possible, the inertia effects at each station. This has been done in a number of ways. The model and balance have been made as light as practical and the bending moments at the strain gauge stations resulting from centrifugal forces have been reduced to low values by counter-balancing (see Fig. 3). Provisions have been made in the front and rear fuselage of the models to mount adjustable ballast in order to minimize the centrifugal bending moment at the front station. A rod carrying a counterweight is connected to the balance between the gauge stations without touching the balance or sting at any point other than the attachment to the balance. In preliminary trials this counterweight was adjusted to bring the centrifugal bending moment at the rear station close to zero. Throughout the tests, the bending moment signals associated with centrifugal forces were small compared to those

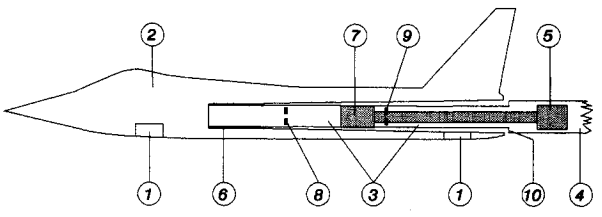

1 provision for ballast
2 HIRM model
3 balance
4 sting
5 counterweight
6 connection balance-model
7 connection balance-counterweight
8 front strain gauge station
9 rear strain gauge station
10 connection balance to sting

Fig. 3 Model-balance assembly.

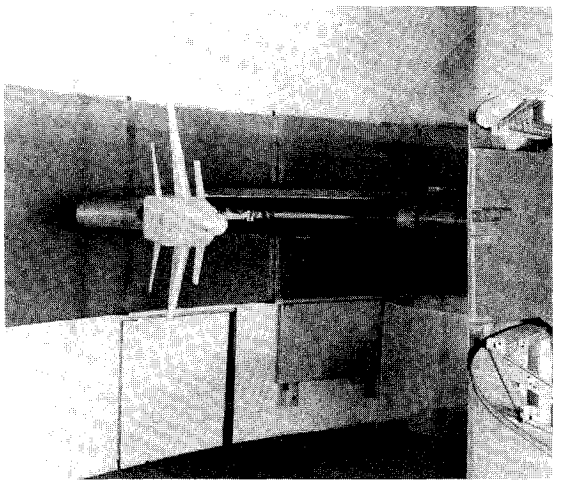

Fig. 4 HIRM I on the whirling arm in the top-in longitudinal mode.

measured in wind-on tests, and the balance-with-counterweight concept was justified.

Figure 4 shows the three-surface HIRM-I model installed on the whirling arm in the top-in longitudinal mode.

Instrumentation

The signals from the strain gauge balance were fed into a signal conditioner. This 8-channel conditioner consisted of amplifiers with a gain set at 960. It contained low-pass filters and since only steady-state measurements were required, the cut-off frequency was set at 2 Hz.

The pressure probes consisted of the pitot-static head mounted in the test passage on the arm opposite the model. For some tests, a calibrated 5-hole nose probe was mounted on the model to give information about the flow conditions near the model.

A "Midas Sirton" computer mounted on a platform near the axis of the whirling arm was the data acquisition computer containing a 12-bit A/D converter. It was connected by way of an RS232C serial link to the "Intellec Superbrain II" microcomputer in the control room. This serial connection ran by way of slip rings mounted on top of the whirling arm. On the microcomputer, software development was carried out for acquisition and preliminary analysis. The data acquisition computer controlled the tests using a program loaded into it from the microcomputer. When the whirling arm was in operation, data could be transferred to the superbrain for inspection and recording. These components are described in greater detail in Ref. 5.

The data as recorded on the microcomputer had to be transferred to a VAX-750 computer for subsequent analysis. Therefore, three different computers were used for data acquisition and analysis and the accompanying difficulties of data transfer between them indicates that a more automated arrangement would be required for routine tests.

Data Reduction and Analysis Method

Since the moment derivatives are usually more important than the force derivatives, only the former will be discussed in this article.

For the longitudinal mode, tests were made with the model in top-in and top-out attitudes corresponding to positive and negative rotation. For each case, wind-on and wind-off tests had to be done with the aerodynamic effects obtained by subtracting wind-off from wind-on balance moments. Assuming a linear relationship between the aerodynamic pitching moment and the pitching angular velocity, the damping-in-pitch derivative can be obtained as follows:

$$C_{m_q} = \frac{\partial C_m}{\partial\left(\frac{q\bar{c}}{V}\right)} = \frac{\Delta C_m}{\Delta\left(\frac{q\bar{c}}{V}\right)} = \frac{C_{m_{\text{top in}}} - C_{m_{\text{top out}}}}{(q_{\text{top in}} - q_{\text{top out}}) \times \frac{\bar{c}}{V}} \tag{1}$$

With $V = q_{\text{top in}} \times R$ (top in refers to the attitude of the model in longitudinal tests, with its wings vertical and its top surfaces towards the center of the whirling arm) and $q_{\text{top in}} = -q_{\text{top out}}$ (top out refers to the attitude of the model in longitudinal tests, with its wings vertical and its top surfaces away from the center of the whirling arm) we obtain

$$C_{m_q} = \frac{(C_{m_{\text{top in}}} - C_{m_{\text{top out}}}) \times R}{2\bar{c}} \tag{2}$$

The parameter $q\bar{c}/V$ is fixed for a given whirling arm and model size for $q\bar{c}/V = (c/R)$. q and V cannot be varied independently and the only way of finding the effect of a change of pitch rate from whirling arm tests on a single model is to reverse the sign of q by a change from top-in to the top-out attitude. It should be noted that $q\bar{c}/V$ rather than q is the parameter determining flow curvature, since physically it represents the difference in angle of attack between two locations longitudinally separated from each other by a distance $\bar{c}$.

For the directional mode, the assessment of the derivatives due to yawing angular velocity is slightly more complex. The balance provides forces and moments about the geometric body axes, but the angular velocity r, as present in the whirling arm directional tests, is about the aerodynamic axes. (The definitions of axes systems are given in Ref. 8). Hence, we have to convert the measured moments to the aerodynamic body axes. For the rolling moment, we have

$$(L)_A = (L)_G \cos(\alpha) + (N)_G \sin(\alpha) \tag{3}$$

(This procedure is also covered in Ref. 9.)

With

$$(C_l)_A = \frac{(L)_A}{\frac{1}{2}\rho V^2 S b} \tag{4}$$

we define

$$(C_{l_r})_A = \frac{\partial (C_l)_A}{\partial\left(\frac{rb}{2V}\right)_A} \tag{5}$$

Due to time limitations, only values for $r = -\omega$ were available from tests with the model in top-up attitude. (Top up refers to the attitude of the model in directional tests, erect with its wings horizontal.) It was therefore necessary to assume that rolling and yawing moments would have been zero for $r = 0$. This assumption was unnecessary if data from top-down tests had been available. With a linear relation between path curvature and the resulting increments in aerodynamic moments, we can derive from the whirling arm experiments

the following stability derivatives:

$$(C_{l_r})_A = \frac{\Delta(C_l)_A}{\Delta\left(\frac{rb}{2V}\right)_A} = \frac{[(C_l)_{\text{top up}} - (C_l)_{r=0}]_A}{-\frac{\omega b}{2V} - 0}$$

$$= -\frac{[(C_l)_A]_{\text{top up}} \times 2V}{\omega b} \tag{6}$$

With $V = \omega \times R$, we get

$$(C_{l_r})_A = -\frac{[(C_l)_A]_{\text{top up}} \times 2R}{b} \tag{7}$$

The derivative $(C_{n_r})_A$ can be obtained analogously.

Supplementary Tests

Before the whirling arm tests were made, some wind-tunnel measurements were made on the light-weight HIRM I to investigate possible scale effects. Such tests were desirable because of the low Reynolds' number at which the whirling arm tests were to be made ($Re_{\bar{c}} = 5.8 \times 10^5$ for HIRM I at test speed, being considerably lower than the Reynolds' numbers of the oscillatory wind-tunnel tests with which they were to be compared). Tests were made at the RAE Bedford facility; 4 × 2.7-m wind tunnel at $Re_{\bar{c}} = 5.0 \times 10^5$ and $Re_{\bar{c}} = 1.1 \times 10^6$. The results, given in Ref. 6, show no significant scale effect for these static tests with similar aerodynamic features at incidences with flow separation. Further checks on scale effects were made with the whirling arm running at only 12 rpm, compared to the usual 25 rpm. (It should be noted that, for the reasons as mentioned before, the effective angular velocity $q\bar{c}/V$ cannot be altered by changing the whirling arm speed. Hence, any difference between the results of tests carried out at different whirling arm speeds should be attributable to Reynolds number effects rather than differences in flow curvature). As shown in Ref. 6, these comparisons did not reveal any clear scale effect. Although such tests did not prove the complete absence of scale effects between the usual whirling arm test Reynolds' numbers and the higher scale wind tunnel and free-flight tests, they did provide confidence that results from the whirling arm could make a significant contribution to knowledge of aircraft behavior at high incidence.

Results

Longitudinal Mode

The pitching moment coefficients obtained from top-out and top-in tests on the whirling arm for HIRM I are given in Fig. 5. In the same figure pitching moments from the wind-tunnel steady-state tests on the same model are shown. The wind-tunnel pitching moments for zero pitching rotation lie between those from the whirling arm for pitch rotations equal in value but opposite in sign. It can be seen that pitching moment must vary with rate of pitch rotation in a linear fashion and that meaningful derivatives can be obtained from the difference between top-out and top-in pitching moments. Such derivatives are shown in Fig. 6 (WA in the figures denotes whirling arm results).

The results of oscillating tests as carried out with the small amplitude oscillatory rig (SAOR) facility[9] are shown as well. This facility, at the RAE Bedford, allows oscillatory testing, subjecting the model to oscillations in pitch rate q and rate of angle-of-attack change ($\dot{\alpha}$). It should be pointed out that the tail-plane angle for the SAOR tests was not zero, but was at settings necessary to limit the load on the sting. Values of C_{m_q} from the whirling arm tests are shown to be almost constant and close to the combined derivative below an incidence of 18 deg. Between 18–26 deg the combined derivative shows a pronounced dip, in effect doubling the pitch damping. There is no similar dip shown by the whirling arm data and it may be concluded that the dip is associated with $\dot{\alpha}$, the rate of change of incidence, in the second part of the combined derivative. Pitching moment derivatives purely associated with the rate of change of incidence are also shown in Fig. 6. These data are obtained from measurements on the acceleration derivative rig (ADR) at RAE Bedford, as described in Ref. 10. In these tests, the model is subjected to a translational oscillation corresponding to changes in angle of attack, with the angular pitching velocity q zero at all times. As can be seen in the figure, these data seem to be corresponding to the earlier mentioned difference between the whirling arm data and the SAOR data.

HIRM II pitching moment coefficients resulting from whirling arm tests and wind-tunnel tests are shown in Fig. 7. Again, we see that the wind-tunnel data are located roughly in the

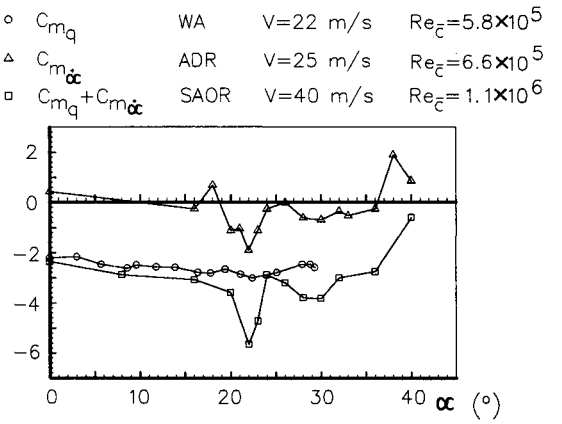

Fig. 6 HIRM I longitudinal stability derivatives.

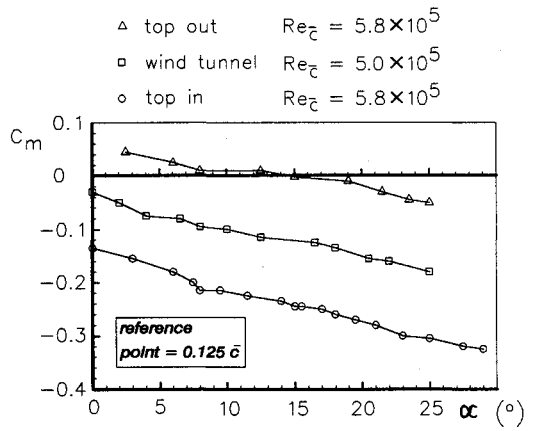

Fig. 5 HIRM I pitching moment coefficients.

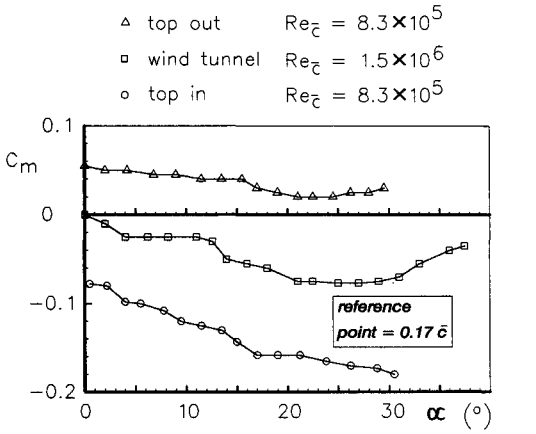

Fig. 7 HIRM II pitching moment coefficients.

middle between top-in and top-out data. The stability derivatives as obtained from Fig. 7 are shown in Fig. 8. Also, this figure contains rotational oscillatory results from large amplitude pitch rig tests[11] (LAPR) as well as translational oscillatory results from ADR tests.[10] (The LAPR facility, like SAOR, allows oscillatory testing, subjecting the model to oscillations in q and $\dot{\alpha}$.) Like the data for HIRM I, the HIRM II curve of C_{m_q} looks smooth, showing little variation with angle of attack. The magnitude of C_{m_q} for this configuration appears to be about half of that of the three-surface configuration, HIRM I. The HIRM II composite derivatives show a sudden "spike," apparently resulting from an $\dot{\alpha}$-effect, present at 17 deg $\leq \alpha \leq$ 20 deg and resulting in a considerable decrease of damping-in-pitch. The difference between the composite derivatives (LAPR data) and whirling arm data are expected to be resulting from $\dot{\alpha}$-effects and the data resulting from ADR tests seem to confirm this.

On the whirling arm the model incidence is unchanged during the measurements. The $\dot{\alpha}$-effects, present only in the oscillatory tests, are related to the buildup of aerodynamic forces as the model incidence is increased. They may arise from interactions between lifting surfaces which may change with onset of vortex flow and burst vortex flow. Their precise cause or nature are not yet understood; the present results and comparisons suggest the following questions:

1) Why is the main $\dot{\alpha}$-effect on HIRM I stabilizing and on HIRM II destabilizing? (i.e., more and less damping in pitch, respectively).

2) Why do the main $\dot{\alpha}$-effects for both models exist only in a particular angle-of-attack range?

Although it is encouraging to see that the results of different techniques seem to complement each other, it should be noted that they do not necessarily have to. This is due to the fact that the flow physics can be quite different for different test techniques, particularly for tests at high angles of attack. At high angles of attack, the results may depend on the earlier-mentioned phenomena such as vortex flow and vortex burst location as function of angle of attack. This dependence on test technique and maneuver input has also been pointed out in Refs. 4 and 10, where tests with different frequencies of oscillations gave different results. A considerable amount of experimental work has been done recently in this area although the wind-tunnel tests were usually on very basic configurations. In this context it is worth mentioning Refs. 12 and 13, where a systematic approach has been made by recording pressure data, strain gauge balance data with visualization in order to try to explain the measured forces and moments by means of the observed flow phenomena.

Directional Mode

Unfortunately, only HIRM I was tested in directional mode, due to lack of time. The HIRM I directional results are presented in Figs. 9 and 10, along with the composite derivatives resulting from SAOR tests.[9] Also, combinations of whirling arm and ADR data are shown. The ADR data were obtained from unpublished preliminary data. Although the comparisons are difficult to make due to different control surface deflections, we see from Figs. 9 and 10 that the composite derivatives as obtained from SAOR tests seem to be roughly equal to the sum of translational (ADR-) results and whirling arm results. From Fig. 10, we see there might be a possible β-effect on yawing moment for angles of attack above 20 deg.

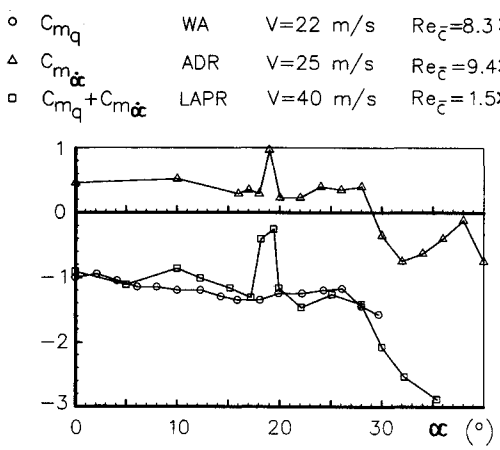

Fig. 8 HIRM II longitudinal stability derivatives.

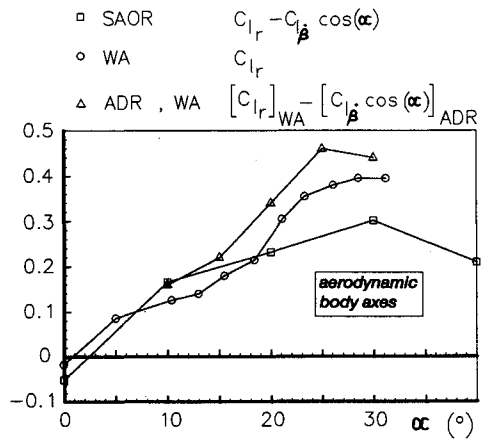

Fig. 9 HIRM I lateral results.

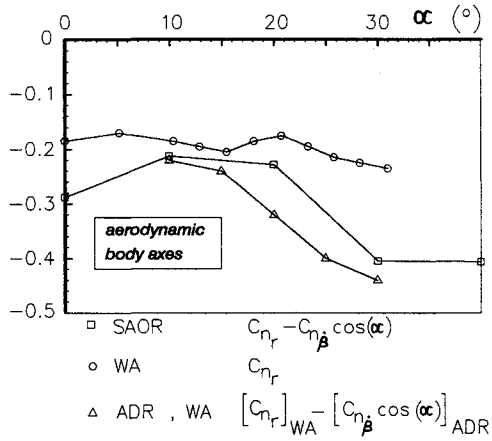

Fig. 10 HIRM I directional results.

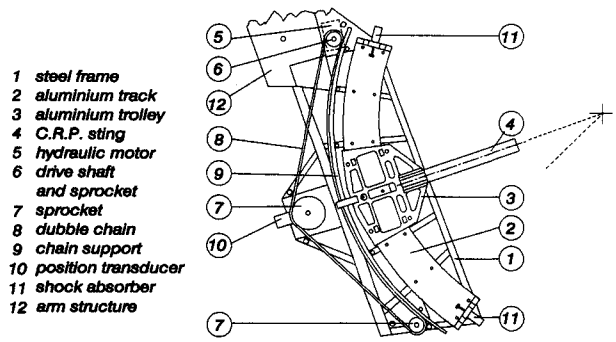

Fig. 11 New $\dot{\alpha}$-rig for transient tests.

Current and Future Developments

To get a better understanding of the effects of rate-of-incidence change on HIRM configurations, a new test rig has been built (Fig. 11) to be mounted on the whirling arm. As in the steady-state experiments, the model will be sting-mounted with an internal strain gauge balance. The light weight sting is mounted on a trolley which can be driven over a solid aluminium crescent-shaped track. This $\dot{\alpha}$-rig will enable tran-

sient tests (not oscillatory) to be made, subjecting the model to a transient and constant rate of incidence change, and aerodynamic forces and moments can be measured during this incidence change. Within limits, it will be possible to independently vary the rate of incidence change and rate of pitch. One possible option will be to arrange a transient motion giving an incidence change with no angular velocity in pitch.

Acknowledgment

This work has been carried out with the support of the Procurement Executive of the Ministry of Defence.

References

[1]Moss, G. F., Ross, A. J., and Butler, G. F., "A Programme of Work on the Flight Dynamics of Departure Using a High Incidence Research Model (HIRM)," Royal Aircraft Establishment, TM Aero 1950, Farnborough, England, UK, July 1982.

[2]Bairstow, L., Bramwell, F. H., and Sillick, W. E. G., "Determination of the Movement of Air in the Whirling Table Shed Due to the Motion of the Whirling Arm With and Without Propellers," Aeronautical Research Committee, R&M 34, London, March 1911.

[3]Halliday, A. S., Bryant, L. W., and Burge, C. H., "The Experimental Determination of Pitching Moment of an Aeroplane Due to Rotation in Pitch," Aeronautical Research Committee R&M 1556, London, March 1933.

[4]Orlik-Rückemann, K. J., "Aerodynamic Aspects of Aircraft Dynamics at High Angles of Attack," *Journal of Aircraft*, Vol. 20, No. 9, 1983, pp. 737–752.

[5]Llewelyn-Davies, D. I. T. P., "The Use of the College of Aeronautics' Whirling Arm Facility to Determine the Effect of Flow Curvature on the Aerodynamic Characteristics of an Ogive-Cylinder Body," Ph.D. Dissertation, College of Aeronautics, Cranfield Inst. of Technology, Cranfield, Bedfordshire, England, UK, July 1987.

[6]Mulkens, M. J. M., and Ormerod, A. O., "Steady-State Experiments for Measurements of Aerodynamic Stability Derivatives of a High Incidence Research Model Using the College of Aeronautics Whirling Arm," College of Aeronautics, Cranfield Inst. of Technology, CoA Rept. 9014, Cranfield, Bedfordshire, England, UK, Aug. 1990.

[7]Ross, A. J., and Edwards, G. F., "Validation of Aerodynamic Parameters for High Incidence Research Models," *Journal of Aircraft*, Vol 26, No. 7, 1989, pp. 621–628.

[8]Hopkin, H. R., "A Scheme of Notation and Nomenclature for Aircraft Dynamics and Associated Aerodynamics," Aeronautical Research Committee R&M 3562, London, 1970.

[9]Ross, A. J., and Reid, G. E. A., "The Development of Mathematical Models for a High Incidence Research Model. Part II: Analysis of Dynamic Test Data," Royal Aerospace Establishment, TR 84072, Farnborough, England, UK, July 1984.

[10]O'Leary, C. O., Weir, B., and Walker, J. M., "Measurement of Derivatives Due to Acceleration in Heave and Sideslip," AGARD Fluid Dynamics Panel Specialists Meeting on Manoeuvring Aerodynamics, Toulouse, France, May 1991; see also: Royal Aerospace Establishmemt, TM Aero 2213, Bedford, England, UK, March 1991.

[11]O'Leary, C. O., and Rowthorne, E. N., "Low Speed Dynamic Tests on a Canard Configured High Incidence Research Model (HIRM 2)," Royal Aerospace Establishment, TR 88024, Farnborough, England, UK, Dec. 1987.

[12]Cunningham, A. M., Jr., and den Boer, R. G., "Low Speed Unsteady Aerodynamics of a Pitching Straked Wing at High Incidence. Part I: Test Program," *Journal of Aircraft*, Vol. 27, No. 1, 1990, pp. 23–30.

[13]Cunningham, A. M., Jr., and den Boer, R. G., "Low Speed Unsteady Aerodynamics of a Pitching Straked Wing at High Incidence. Part II: Harmonic Analysis," *Journal of Aircraft*, Vol. 27, No. 1, 1990, pp. 31–41.